ISBN: 978-3-95450-214-1 ISSN: 2673-5490 doi:10.18429/JACoW-IPAC2021-MOPAB063

COMMISSIONING STRATEGY FOR DIAMOND-II

M. Apollonio*, MAX IV Laboratory, Lund University, Lund, Sweden
R. Fielder, H. Ghasem, I. P. S. Martin, Diamond Light Source, Oxfordshire, UK

Abstract

At Diamond Light Source we are working on the upgrade towards a machine aimed at a factor 20 reduction in emittance and an increase of the capacity for beamlines. Crucially the success of the programme depends on the ability to inject and capture the electrons in the storage ring, and finally reach control of beam alignment and the linear optics. The paper presents the series of strategies adopted to achieve the commissioning of the machine, from the threading procedure ensuring the first turn of the electron beam, to the orbit corrections in the storage ring. Beam based alignment of the quadrupoles and skew quadrupoles is illustrated and restoration of the linear optics (LOCO) for the storage ring is presented. Main performance parameters (Dynamic Apertures, Injection Efficiency and Lifetime) are calculated to evaluate the performance of the commissioned lattices.

INTRODUCTION

Low emittance lattices with high gradients and therefore more sensitive to magnet errors, call for a full realistic modelling of all the aspects up to the operational phase of a machine. In the last decade it became apparent how a realistic simulation is fundamental not only in the design phase of a lattice but also in the prediction of its performance during the inception stages of commissioning. This need emerged during the CDR [1] and Machine Advisory Committee (MAC) stages of Diamond-II [2] and as such we devoted our efforts to introduce a structured procedure to study this process, that facilitates calculations with many error seeds.

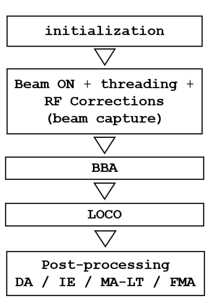

Figure 1: Block diagram representing the sequence of steps used to characterize the commissioning of Diamond-II.

SIMULATED COMMISSIONING

Given the extensive use of MATLAB [3] and AT2 [4], the whole Diamond-II commissioning strategy is based on the Simulated Commissioning (SC) toolkit [5, 6]. The code lends itself well to a start-to-end characterization of the commissioning procedure with the possibility of introducing ad hoc sections, like:

- Beam based alignment (BBA),
- Linear Optics Corrections (LOCO),
- Post-processing of the machine performance.

It is also easy to break down the entire procedure in modular blocks that facilitate processing and debugging. Figure 1 illustrates the main elements of the commissioning procedure as implemented for Diamond-II.

Machine Errors

The set of errors at Diamond-II has been refined since the early stages of the CDR, and also thanks to the input and suggestions of the international panel at the MAC meetings. Table 1 summarizes the RMS errors (truncated at 2σ) currently adopted in our design, that are inserted in the model and constitute the starting point to define a realistic lattice. A realistic injected beam as coming from the booster complements this information (see Table 2).

Table 1: Diamond-II Errors for Quadrupoles, Sextupoles, Octupoles, Dipoles (L/Q), Anti-Bends, Girders, BPMs and Corrector Magnets (CM). Note the Different BPM Noise at Low Current Turn-by-Turn Mode (tbt), and in Closed Orbit Mode (co)

element	**δx,y (μm)**	**δroll (μrad)**	**calib (%)**	**noise tbt [co] (μm)**	**limit (mrad)**
Q/S/O	35	100	0.1	-	-
DL	100	100	0.05	-	-
DQ/AB	50	100	0.05	-	-
GIRD	150	150	-	-	-
BPM	500	150	5	60 [1]	-
CM	-	150	5	-	1

Table 2: Injected Beam Parameters for a Beam Matched to SR Optics

Diamond-II booster beam parameters	
ϵ_x (nm)	17.7
ϵ_y (nm)	1.77
$\Delta E/E$ (%)	0.086
σ_L (mm)	11.61

Initialisation and Error Implementation

In this step an AT2 lattice file for the storage ring (SR) is uploaded, and the commissioning parameters described in the previous section are implemented in the machine. The

* marco.apollonio@maxiv.lu.se

ISBN: 978-3-95450-214-1 ISSN: 2673-5490 doi:10.18429/JACoW-IPAC2021-MOPAB063

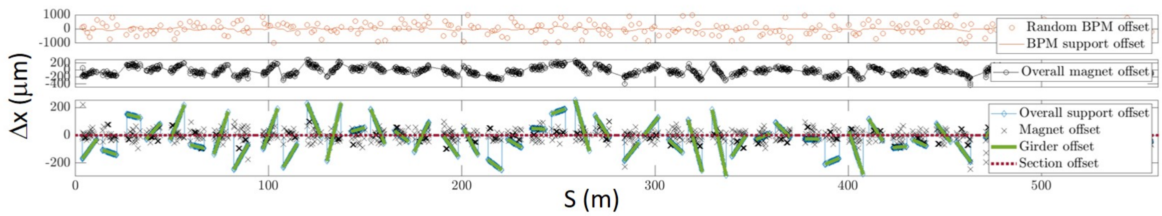

Figure 2: Implementation of errors in the horizontal plane: (top) position errors for the BPMs, (centre) position uncertainty of the magnets, (bottom) motion of girders (green segments), with their clear sway and yaw movements.

implementation of errors can be graphically monitored, as illustrated in Fig. 2, where the displacements in the horizontal plane for BPMs, girders and magnet mounted on girders are shown. Similar plots show moves in the vertical plane and the roll around the longitudinal direction.

Beam On: Injection and RF Optimisation

This bloc mimics the steps needed to inject the first beam and thread it through the storage ring until a multi-turn condition is established, after which an optimisation of the RF cavity working point is attempted. In order to avoid the strong non-linearities and orbit distortions created by the initial large errors on magnets and BPMs, all the sextupoles are initially set to zero current and the RF is switched off. Figure 3 shows a typical threading sequence on a set of 100 electrons, for an on-axis injection at low current, where correctors are varied according to a 1-turn response matrix (RM) with a large Tikhonov regularization parameter (α_T=50) to keep the corrector magnets below their maximal amplitude (1 000 µrad). The threading is repeated with a 2-turn RM, after which sextupoles are gradually set back to their nominal working point. Finally, the RF is restored, which is usually enough to experience a substantial change in the maximal number of turns. A scan on the RF frequency and phase against the average displacement of the trajectory is then done to find a better working point. This is illustrated in Fig. 4, where 100 electrons are monitored in the longitudinal

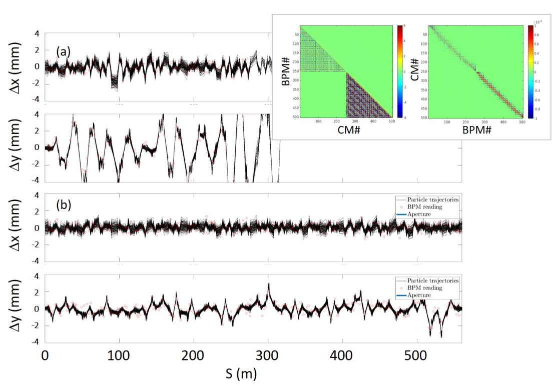

Figure 3: First turn threading in the Diamond-II SR. (Top) initial attempt with total loss of the beam, (bottom) 1^{st} turn transmission completed with beam ready for a 2-turn threading. Inset: 1-turn RM and its pseudo-inverse.

phase space for 1000 turns. Correctly setting the RF voltage, phase and frequency allows a 100% transmission over 10000 turns. At this stage the closed orbit condition is typically reached, and it is possible to move on with the centring of the magnetic elements in the SR, as described in the next section.

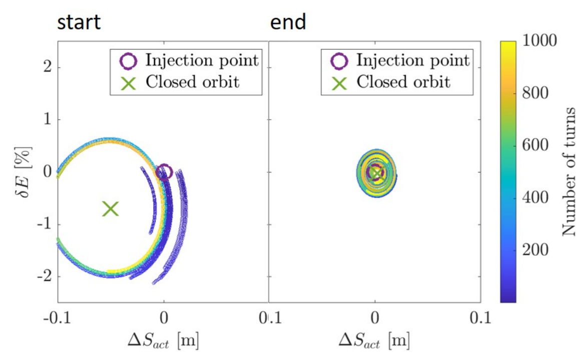

Figure 4: Optimisation of the RF working point as seen in the longitudinal phase space. The starting point (left) shows a poor transmission through the SR (broken blue lines), which is dramatically improved with the new settings (right).

Beam Based Alignment

The steps seen so far are sufficient to reach a closed orbit with an on-axis injection allowing a low current of 0.3 mA in the SR. Initial attempts at trying an off-axis injection at -5 mm, do not seem successful, which is mainly due to the magnitude of errors. Such a low current in the SR entails a large uncertainty at the BPM readings, quantified as 60 µm (see Table 1). Despite this limitation we proceeded with the beam-based alignment (BBA), to try and reduce the initially large offset at the BPMs (500 µrad RMS). In the simulated commissioning of Diamond-II we have explored the two cases of a standard quadrupole-centring technique, and a centring based on the skew quadrupoles embedded in the sextupoles (skew-centring), the latter technique resting upon a perfect alignment between the magnetic centres of the two multipoles. Figure 5 illustrates the set-up of magnets involved in the skew-centring procedure. The entire process has been made human intervention free and relies on a progressive reduction of the Tikhonov regularization parameter from large values (α_T=35) to 0, in the attempt of keeping low CM strengths at the beginning of the process, when the

12th Int. Particle Acc. Conf. IPAC2021, Campinas, SP, Brazil JACoW Publishing
ISBN: 978-3-95450-214-1 ISSN: 2673-5490 doi:10.18429/JACoW-IPAC2021-MOPAB063

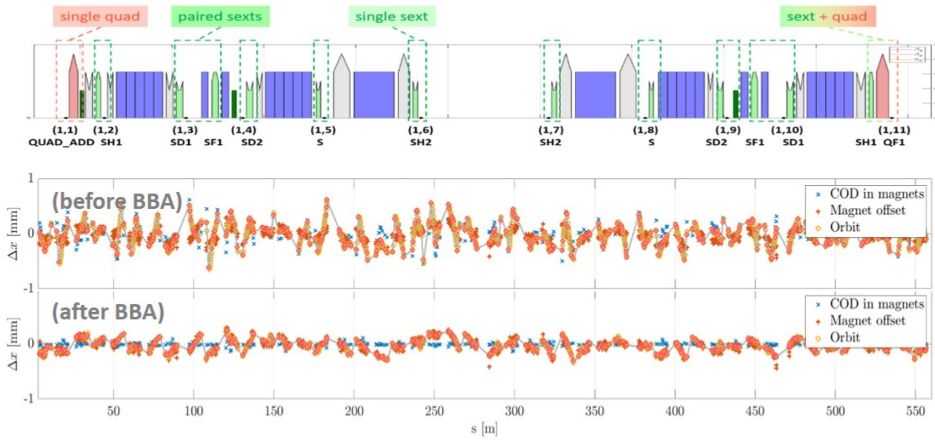

Figure 5: Skew-centring BBA at Diamond-II: (top) pairing between BPMs and magnets, showing BPM to quadrupole (red), BPM to sextupole (green), BPM to two sextupoles and BPM to a quadrupole and a sextupole couplings. (Bottom) effect of BBA seen on the horizontal orbit before and after the procedure, with the final orbit closely following the pattern of misaligned girders.

offsets at the BPMs are still very large. CM strengths and residuals at BPMs are monitored during the procedure, commanding the centring of the more troublesome cells. It was noted that the convergence of α_T depends on the magnitude of the errors and is particularly sensitive to the uncertainty in the dipole position. As such, the alignment tolerance for the gradient dipoles and anti-bend magnets has been tightened from 100 µm to 50 µm (see Table 1). Preliminary studies indicate that, with this limitation, orbit and optics correction can be reliably achieved for α_T=0.

Restoring Linear Optics

Once an acceptable control of the orbit in the machine has been reached, we attempt at restoring the SR linear optics, making use of the well-known code LOCO [7]. The optimisation can be launched from within the SC-toolkit which exits three 'ring' outputs: the ideal machine (prior to any error introduction), the spoiled lattice (after full error implementation and BBA corrections), the restored lattice (after LOCO). This structure makes it easy to proceed to the next stage, where a thorough calculation of the main SR performance parameters is executed.

Post-processing

As anticipated in the previous section, three configurations of the ring are available after linear optics corrections, that can be passed through the calculation of observables characterizing the performance of the SR, namely: Dynamic Aperture (DA), Injection Efficiency (IE) and Momentum Aperture (MA) with Touschek Lifetime. Figure 6 shows a three error seeds calculation of DA and IE for Diamond-II, comparing the ideal SR, the pre-loco case and the post-loco configuration. The applied LOCO corrections improve the performance of the lattice. The red shaded area represents the envelope of a 20 seed simulation performed with the code elegant [2, 8] in the lattice development studies, using

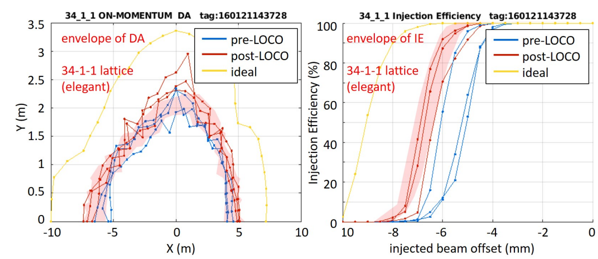

Figure 6: Diamond-II SR DA (left) and IE (right) calculated for an ideal machine (yellow line), for a spoiled machine prior to LOCO corrections (blue lines for 3 error seeds) and after LOCO (red lines). The red shade shows the envelope of 20 seeds calculations done with elegant.

a reduced error set to bypass the BBA and LOCO steps, indicating a good agreement between the two procedures.

CONCLUSIONS

The strategy adopted at Diamond-II for the commissioning of the SR is based on the SC-toolkit. A BBA section has been developed which is specific for the machine, relying either on a standard quadrupole-centring or on a skew-centring technique. LOCO and subsequent post-processing show encouraging results. Future developments include a better understanding of LOCO optimisation with anti-bend lattices, and the development of a strategy to deal with the alignment of the anti-bends.

ACKNOWLEDGEMENTS

The authors are particularly grateful to Thorsten Hellert for the thorough and clarifying discussions on the use of the SC-toolkit. M. Apollonio is grateful to Diamond former colleagues for the kind cooperation in the preparation of this document.

ISBN: 978-3-95450-214-1 ISSN: 2673-5490 doi:10.18429/JACoW-IPAC2021-MOPAB063

REFERENCES

[1] "Diamond-II Conceptual Design Report", Diamond Light Source, https://www.diamond.ac.uk/Home/About/Vision/Diamond-II.html

[2] H. Ghasem, I.P.S. Martin, B. Singh, and R.P. Walker, "Progress with the Diamond-II Storage Ring Lattice", in *Proc. IPAC'21*, Campinas, Brazil, May 2021, paper THPAB090, this conference.

[3] MATLAB, version 9.8.0 (R2020a) Natick, Massachussets: The MathWorks Inc. 2020, https://in.mathworks.com/.

[4] Accelerator Toolbox Collaboration, http://atcollab.sourceforge.net/.

[5] T. Hellert, P. Amstutz, C. Steier, and M. Venturini, "Toolkit for simulated commissioning of storage-ring light sources and application to the advanced light source upgrade accumulator", *Phys. Rev. Accel. Beams*, vol. 22, no. 10, Oct. 2019. doi:10.1103/physrevaccelbeams.22.100702

[6] T. Hellert, SC manual, https://sc.lbl.gov/main.html

[7] J. Safranek, "Experimental determination of storage ring optics using orbit response measurements", *Nucl. Inst. and Meth.*, vol. 388, no. 1–2, pp. 27–36, Mar. 1997. doi:10.1016/s0168-9002(97)00309-4

[8] M. Borland, "ELEGANT: A Flexible SDDS-Compliant Code for Accelerator Simulation", APS report No. LS-287, Sep. 2000. doi:10.2172/761286